Supplementary Information — Photooxidation of PC$_{60}$BM: New Insights from Spectroscopy

Iulia Emilia Brumboiu[a),b)],[1,2] Leif KE Ericsson[a)],[3] Vanja Blazinic,[3] Rickard Hansson,[3] Andreas Optiz,[4] Barbara Brena,[2] and Ellen Moons[3]

[1)] *Department of Theoretical Chemistry and Biology, KTH Royal Institute of Technology, SE-10691 Stockholm, Sweden*

[2)] *Department of Physics and Astronomy, Uppsala University, SE-75120 Uppsala, Sweden*

[3)] *Department of Engineering and Physics, Karlstad University, SE-65188 Karlstad, Sweden*

[4)] *Institut für Physik, Humbolt Universität zu Berlin, 12489 Berlin, Germany*

(Dated: 16 September 2022)

Included here are: **a)** the molecular structures of possible PC$_{60}$BM photodegradation products; **b)** the calculated C1s near edge X-ray absorption fine structure (NEXAFS) spectrum of a PC$_{60}$BM molecule with two OH groups attached to the fullerene cage; calculated **c)** infrared (IR), **d)** C1s X-ray photoelectron spectroscopy (XPS), **e)** O1s XPS, **f)** C1s NEXAFS, **g)** O1s NEXAFS spectra of all the photodegradation products; **h)** a comparison between the calculated IR spectra of PC$_{60}$BM-anhydride, PC$_{58}$BM-anhydride, PC$_{60}$BM-dicarbonyl and PC$_{58}$BM-dicarbonyl.

[a)] These authors have contributed equally.

[b)] Current address: Faculty of Physics, Astronomy and Informatics, Nicolaus Copernicus University, 87-100 Toruń, Poland.

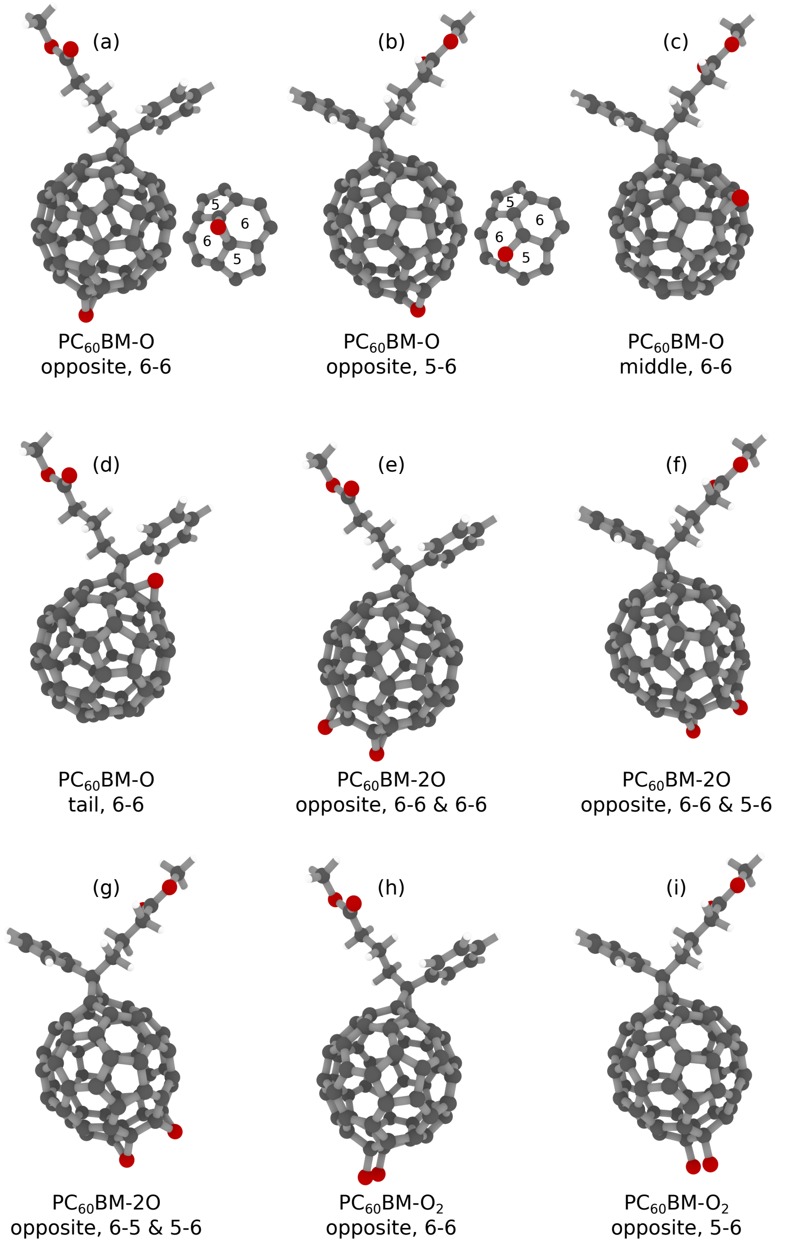

FIG. S1. Relaxed molecular structures of possible PC$_{60}$BM photodegradation products involving oxygen. C atoms are depicted in gray, O in red and H in white. If the oxygen adsorption site is at the intersection of two hexagons, the structure is denoted 6–6, while adsorption at the intersection between a hexagon and a pentagon is denoted 5–6. Examples of 6–6 and 5–6 adsorption sites are shown in the insets to (a) and (b).

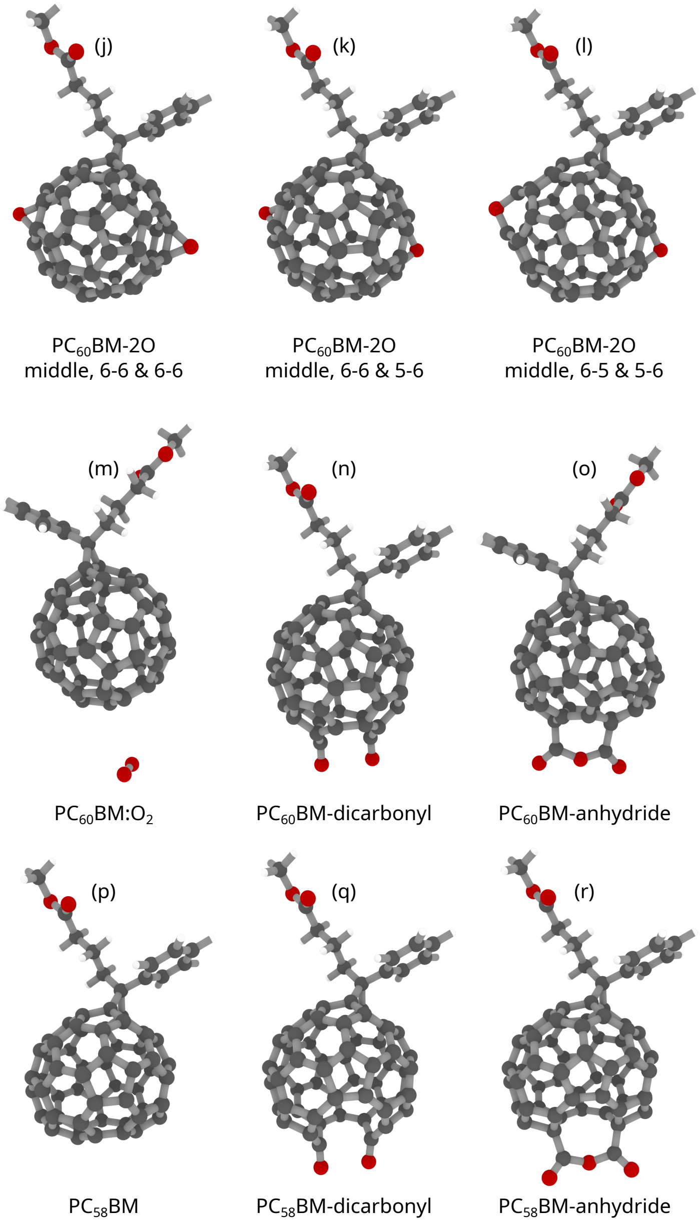

$PC_{60}BM$-2O middle, 6-6 & 6-6

$PC_{60}BM$-2O middle, 6-6 & 5-6

$PC_{60}BM$-2O middle, 6-5 & 5-6

$PC_{60}BM:O_2$

$PC_{60}BM$-dicarbonyl

$PC_{60}BM$-anhydride

$PC_{58}BM$

$PC_{58}BM$-dicarbonyl

$PC_{58}BM$-anhydride

FIG. S2. (Continued) Relaxed molecular structures of possible $PC_{60}BM$ photodegradation products involving oxygen.

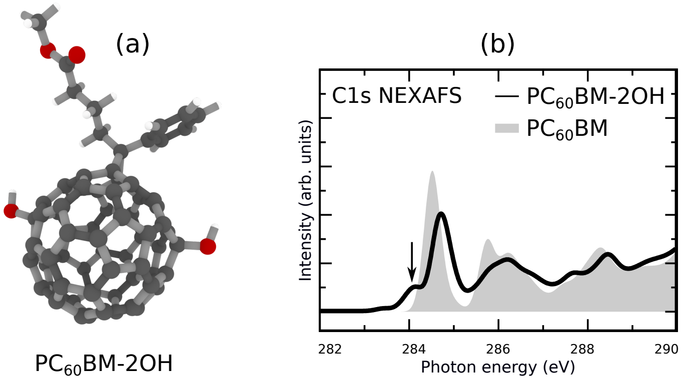

PC$_{60}$BM-2OH

FIG. S3. (a) Molecular structure and (b) calculated C1s NEXAFS spectrum of a PC$_{60}$BM molecule with two OH groups attached to the fullerene cage (black line), shown in comparison to the calculated spectrum of pristine PC$_{60}$BM (shaded gray area, from Ref. [1]). The NEXAFS spectra have been shifted by 2.05 eV towards higher photon energies, a shift required to align the pristine PC$_{60}$BM calculated π^* peak to the experimentally measured one for unexposed PC$_{60}$BM.

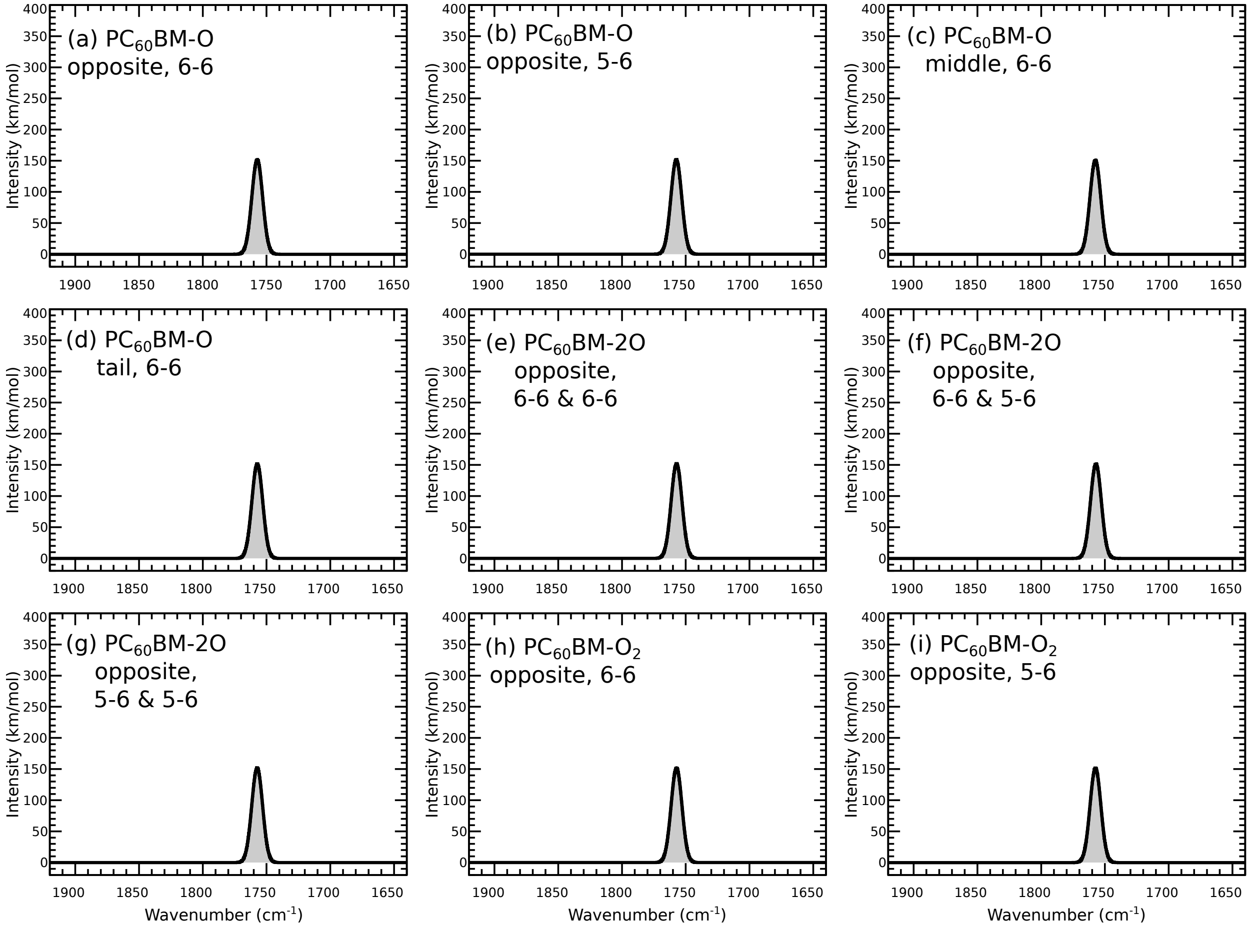

FIG. S4. Calculated IR spectra of the degradation products depicted in Fig. S1 (a)–(i) (black line), shown in comparison to the calculated spectrum of pristine $PC_{60}BM$ (shaded gray area). All spectra have been scaled by a factor 0.9627[2] and shifted by 22 cm^{-1} toward lower wavenumbers, a shift required to align the pristine $PC_{60}BM$ carbonyl peak to the experimentally measured one for unexposed $PC_{60}BM$. The spectra are obtained by broadening the calculated bar graphs with Gaussian functions of 10 cm^{-1} FWHM.

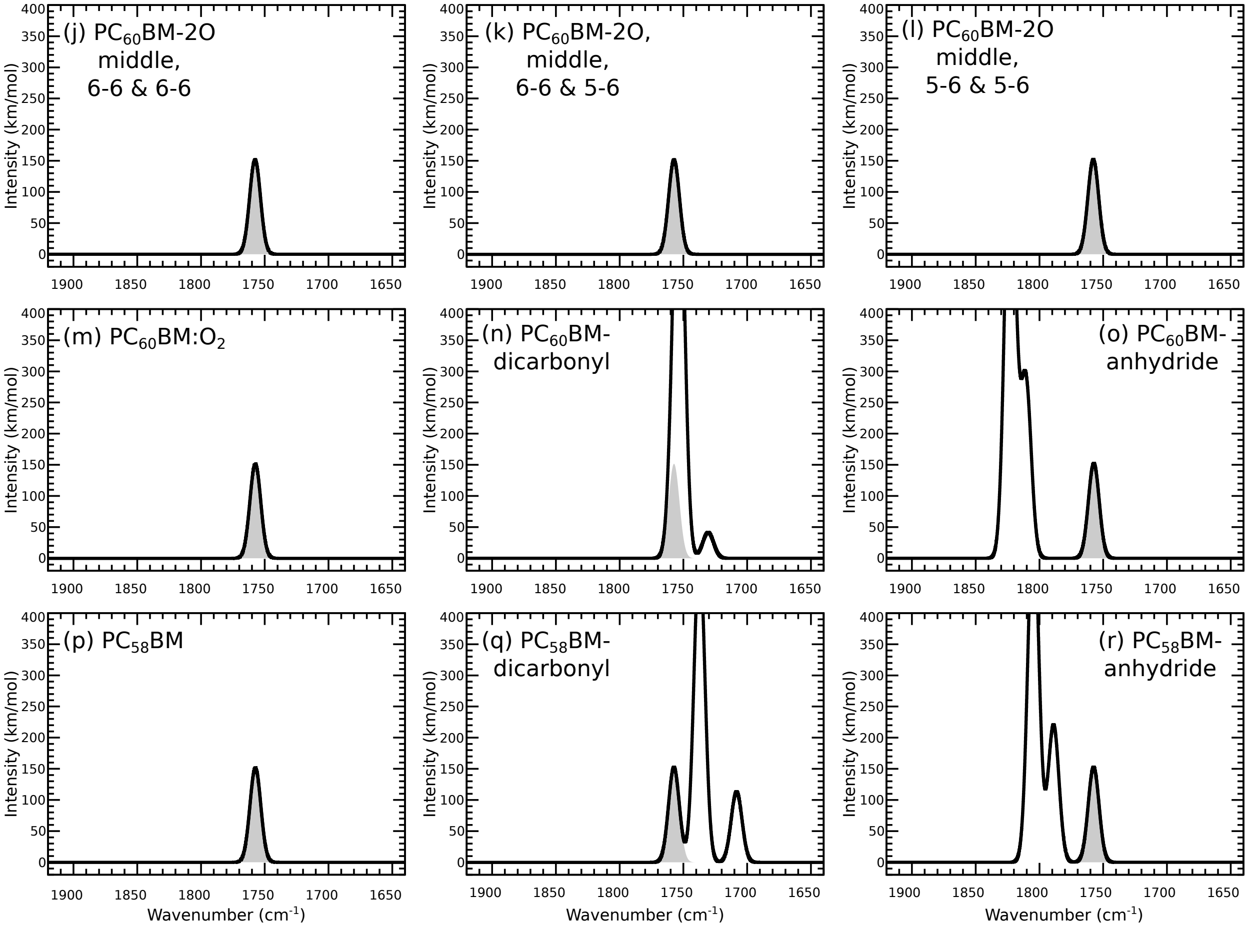

FIG. S5. Calculated IR spectra of the degradation products depicted in Fig. S2 (j)–(r) (black line), shown in comparison to the calculated spectrum of pristine $PC_{60}BM$ (shaded gray area). All spectra have been scaled by a factor 0.9627[2] and shifted by 22 cm^{-1} toward lower wavenumbers, a shift required to align the pristine $PC_{60}BM$ carbonyl peak to the experimentally measured one for unexposed $PC_{60}BM$. The spectra are obtained by broadening the calculated bar graphs with Gaussian functions of 10 cm^{-1} FWHM.

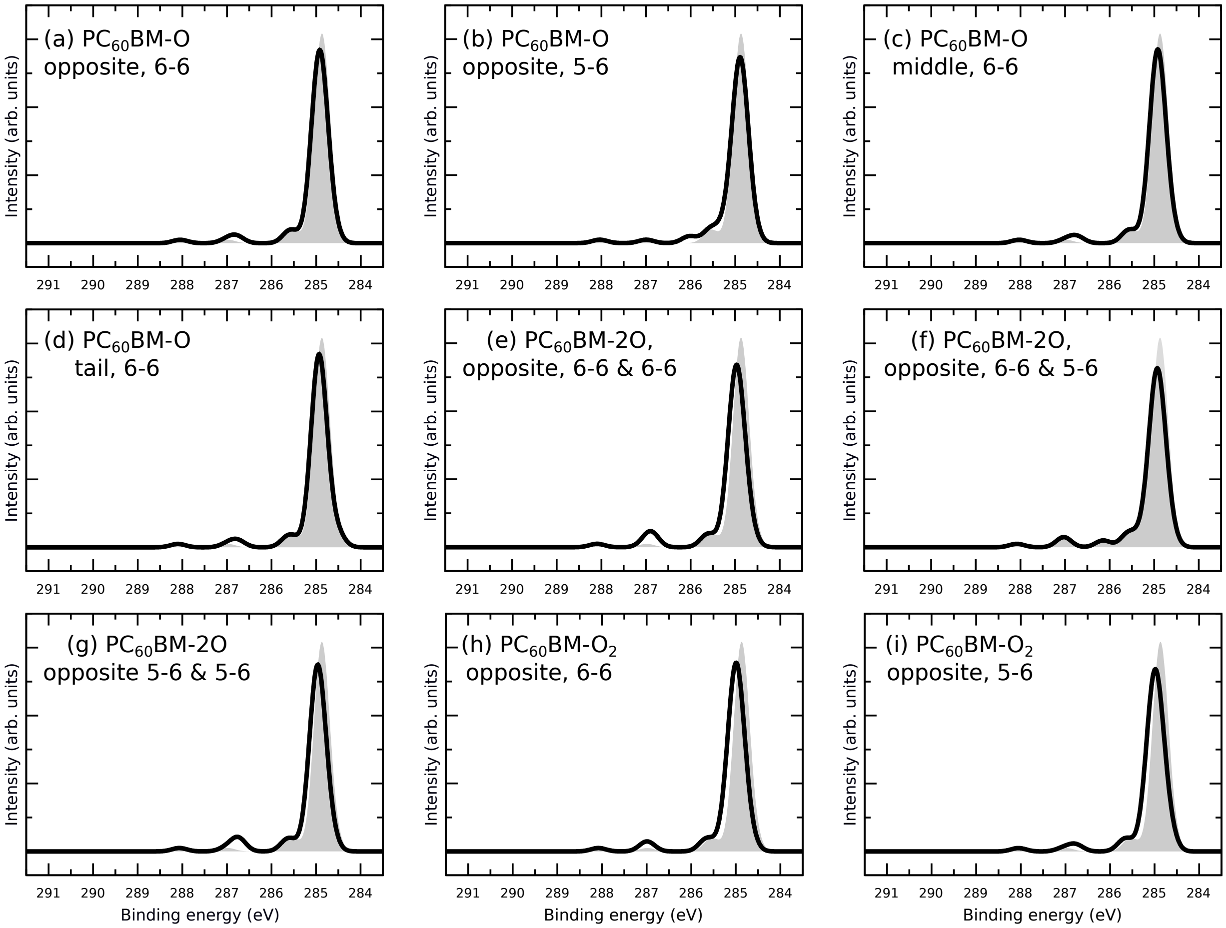

FIG. S6. Calculated C1s XPS spectra of the degradation products depicted in Fig. S1 (a)–(i) (black line), shown in comparison to the calculated spectrum of pristine $PC_{60}BM$ (shaded gray area). All spectra have been shifted by 5 eV towards lower binding energies, a shift required to align the pristine $PC_{60}BM$ calculated XPS spectrum to the experimentally measured one for unexposed $PC_{60}BM$. The spectra are obtained by broadening the calculated bar graphs with Gaussian functions of 0.5 eV FWHM.

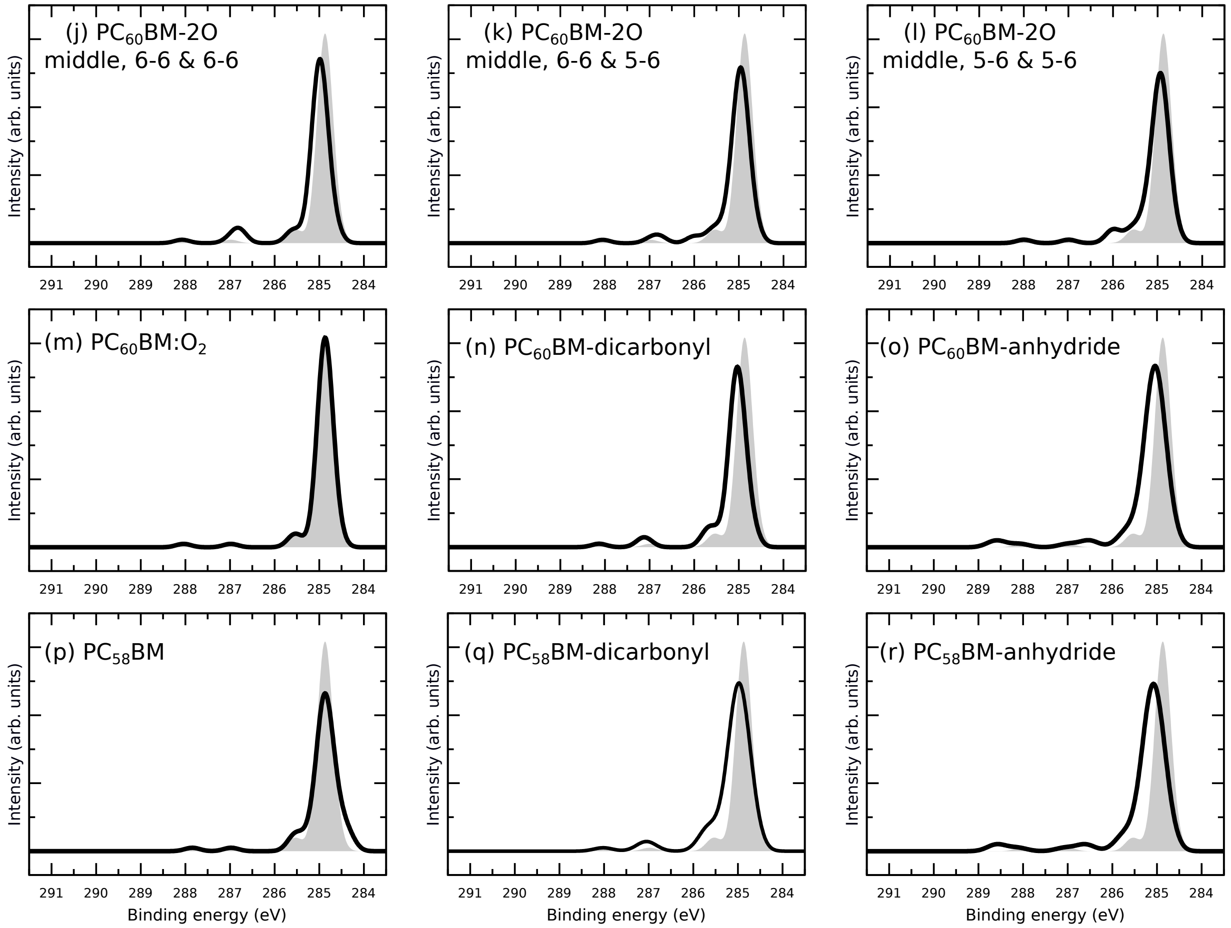

FIG. S7. Calculated C1s XPS spectra of degradation products depicted in Fig. S2 (j)–(r) (black line), shown in comparison to the calculated spectrum of pristine $PC_{60}BM$ (shaded gray area). All spectra have been shifted by 5 eV towards lower binding energies, shift required to align the pristine $PC_{60}BM$ calculated XPS spectrum to the experimentally measured one for unexposed $PC_{60}BM$. The spectra are obtained by broadening the calculated bar graphs with Gaussian functions of 0.5 eV FWHM.

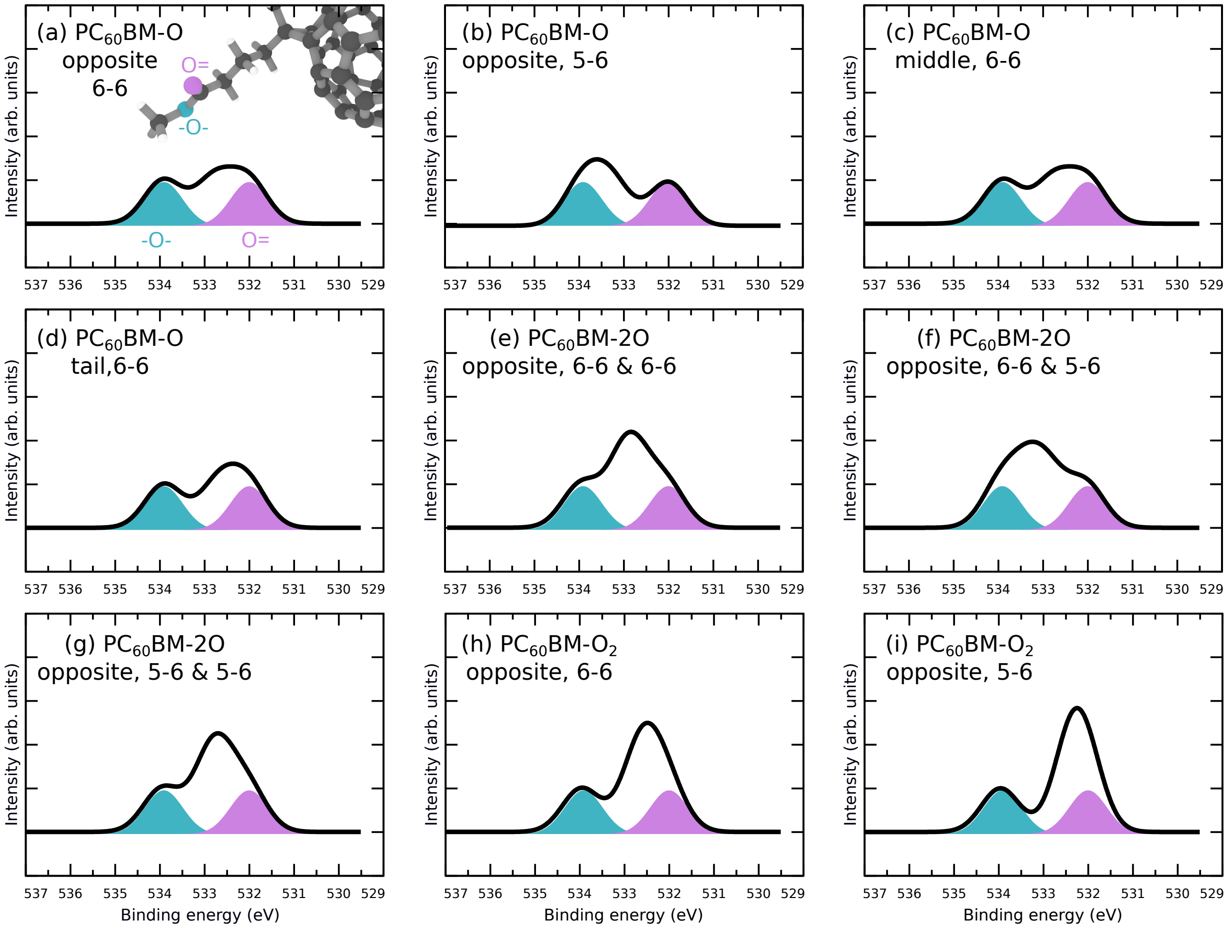

FIG. S8. Calculated O1s XPS spectra, from Ref. [3], of the degradation products depicted in Fig. S1 (a)–(i) (black line), shown in comparison to the calculated spectrum of pristine PC$_{60}$BM (shaded area). The components of the pristine PC$_{60}$BM spectrum are shown in purple (double bonded oxygen, O=) and blue (single bonded oxygen, –O–), corresponding to the colors used to depict the side-chain oxygen atoms in the inset to (a). All spectra have been shifted by 4.7 eV towards lower binding energies, a shift required to align the pristine PC$_{60}$BM calculated O= peak to the experimentally measured low binding energy XPS peak of unexposed PC$_{60}$BM. The spectra are obtained by broadening the calculated bar graphs with Gaussian functions of 1.0 eV FWHM.

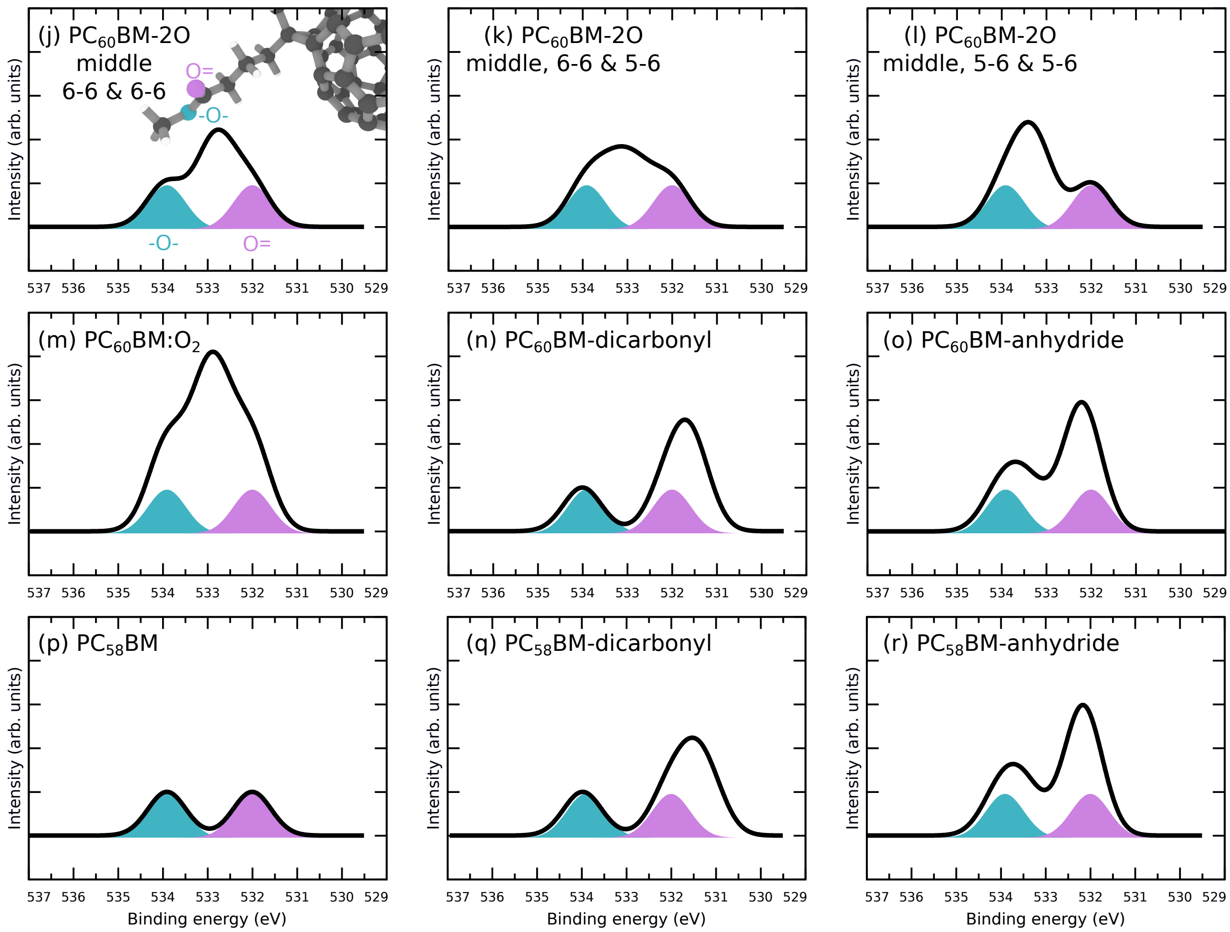

FIG. S9. Calculated O1s XPS spectra of the degradation products depicted in Fig. S2 (j)–(r) (black line), shown in comparison to the calculated spectrum of pristine $PC_{60}BM$ (shaded area). The components of the pristine $PC_{60}BM$ spectrum are shown in purple (double bonded oxygen, O=) and blue (single bonded oxygen, –O–), corresponding to the colors used to depict the side-chain oxygen atoms in the inset to (a). All spectra have been shifted by 4.7 eV towards lower binding energies, a shift required to align the pristine $PC_{60}BM$ calculated O= peak to the experimentally measured low binding energy XPS peak of unexposed $PC_{60}BM$. The spectra are obtained by broadening the calculated bar graphs with Gaussian functions of 1.0 eV FWHM. The spectra in (j)–(m) are from Ref. [3].

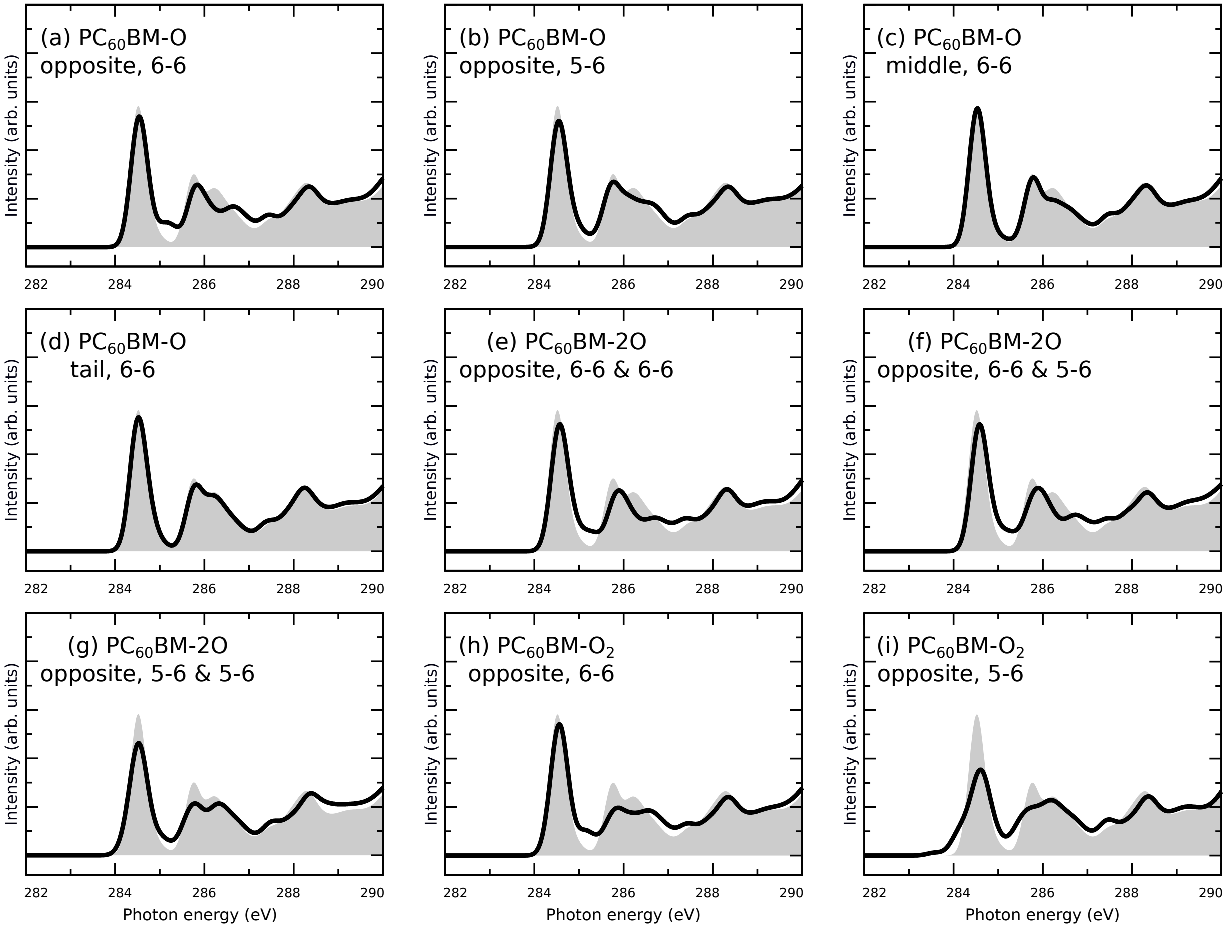

FIG. S10. Calculated C1s NEXAFS spectra of the degradation products depicted in Fig. S1 (a)–(i) (black line), shown in comparison to the calculated spectrum of pristine $PC_{60}BM$ (shaded gray area, from Ref. [1]). All spectra have been shifted by 2.05 eV towards higher photon energies, a shift required to align the pristine $PC_{60}BM$ calculated π^* peak to the experimentally measured one for unexposed $PC_{60}BM$.

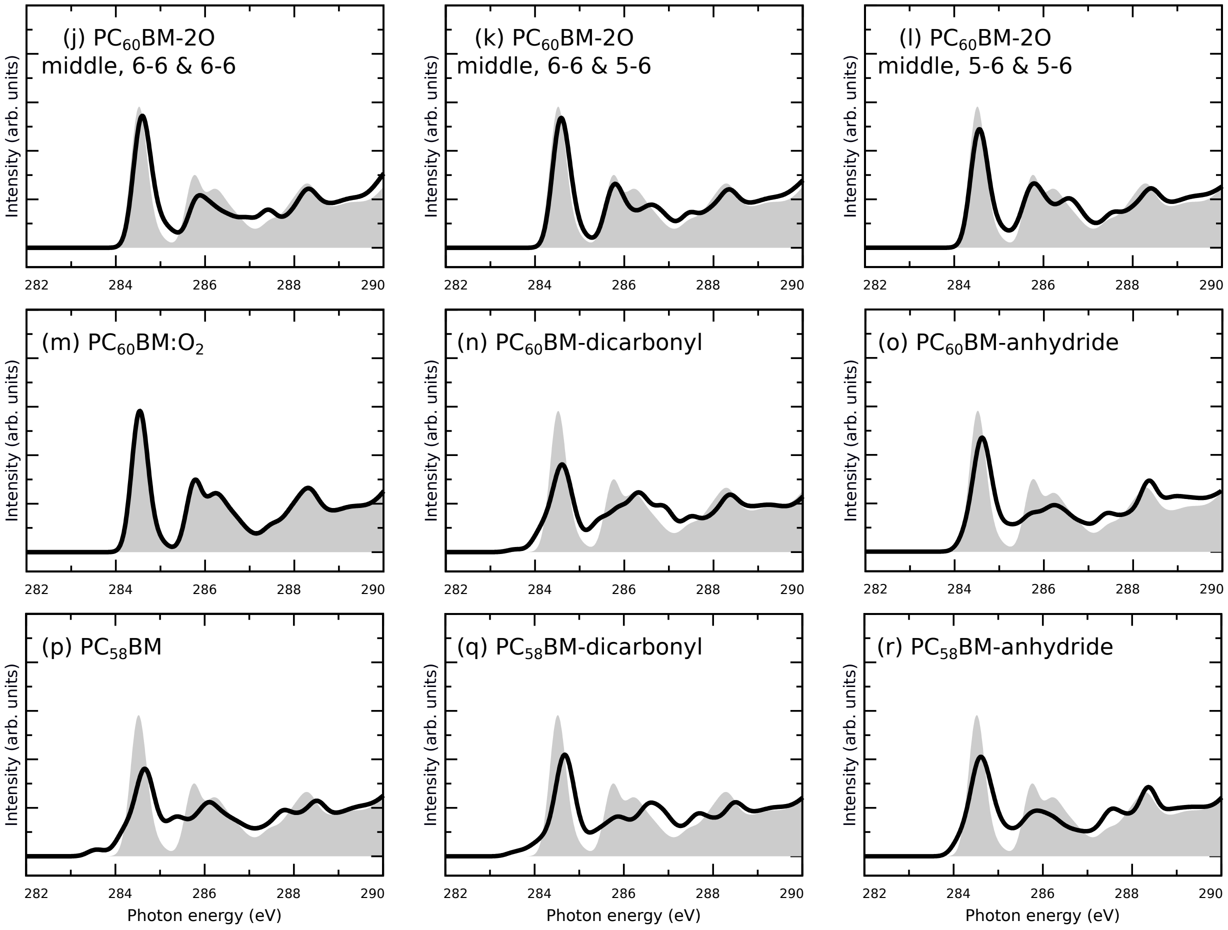

FIG. S11. Calculated C1s NEXAFS spectra of the degradation products depicted in Fig. S2 (j)–(r) (black line), shown in comparison to the calculated spectrum of pristine $PC_{60}BM$ (shaded gray area, from Ref. [1]). All spectra have been shifted by 2.05 eV towards higher photon energies, a shift required to align the pristine $PC_{60}BM$ calculated π^* peak to the experimentally measured one for unexposed $PC_{60}BM$.

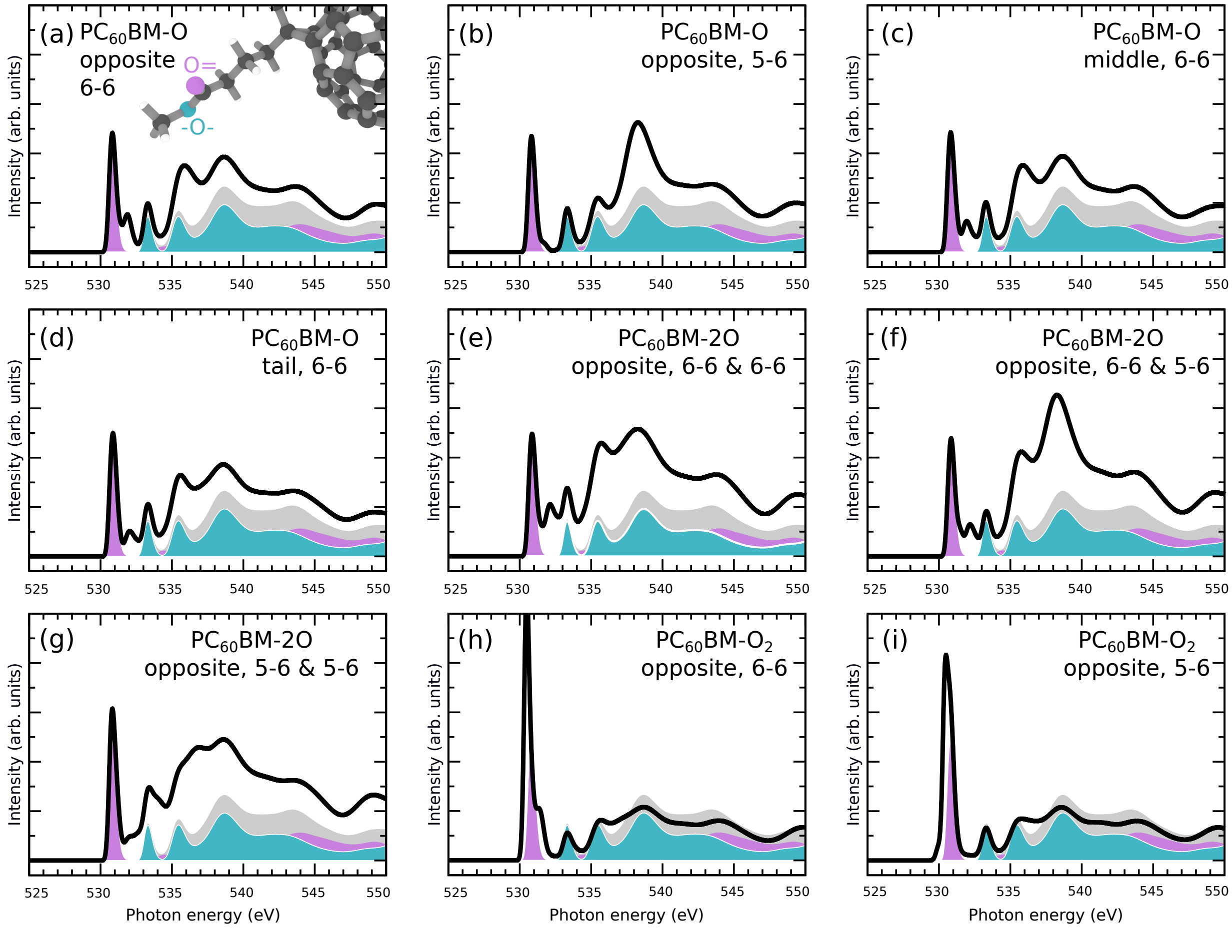

FIG. S12. Calculated O1s NEXAFS spectra, from Ref. [3], of the degradation products depicted in Fig. S1 (a)–(i) (black line), shown in comparison to the calculated spectrum of pristine $PC_{60}BM$ (shaded gray area). The components of the pristine $PC_{60}BM$ spectrum are shown in purple (double bonded oxygen, O=) and blue (single bonded oxygen, –O–), corresponding to the colors used to depict the side-chain oxygen atoms in the inset to (a). All spectra have been shifted by 0.8 eV towards lower photon energies, shift required to align the pristine $PC_{60}BM$ calculated π^* peak to the experimentally measured one for unexposed $PC_{60}BM$.

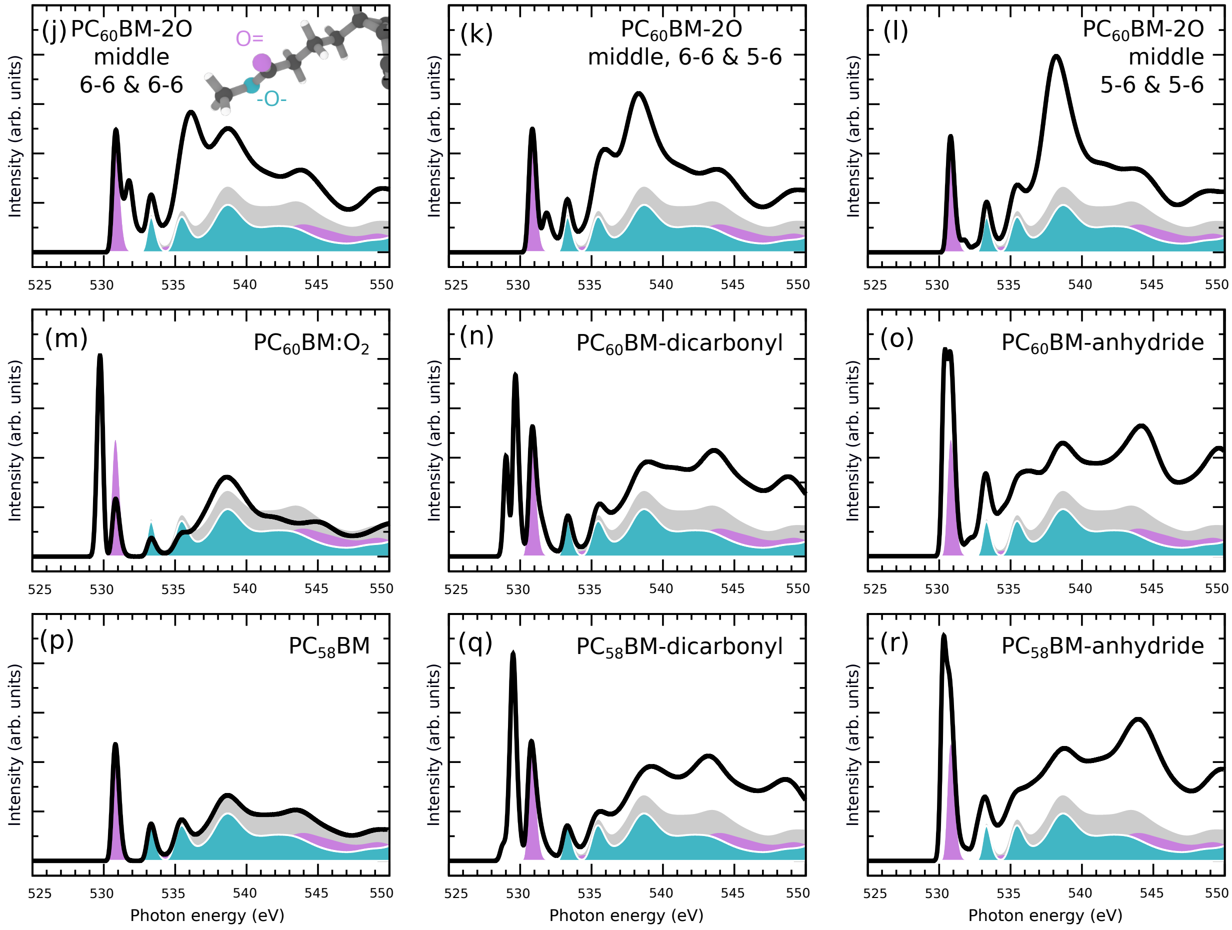

FIG. S13. Calculated O1s NEXAFS spectra of the degradation products depicted in Fig. S2 (j)–(r) (black line), shown in comparison to the calculated spectrum of pristine $PC_{60}BM$ (shaded gray area). The components of the pristine $PC_{60}BM$ spectrum are shown in purple (double bonded oxygen, O=) and blue (single bonded oxygen, –O–), corresponding to the colors used to depict the side-chain oxygen atoms in the inset to (a). All spectra have been shifted by 0.8 eV towards lower photon energies, shift required to align the pristine $PC_{60}BM$ calculated π^* peak to the experimentally measured one for unexposed $PC_{60}BM$. The spectra in (j)–(m) are from Ref. [3].

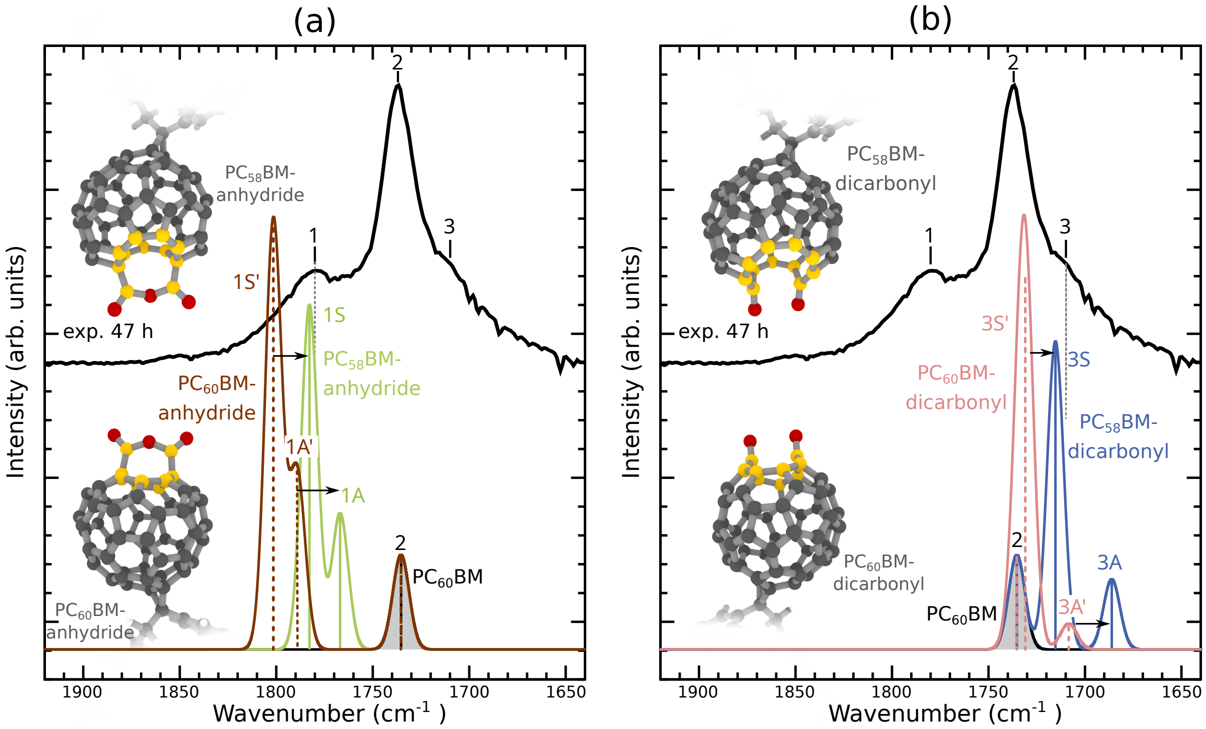

FIG. S14. Calculated IR spectra of (a) PCBM-anhydride and (b) PCBM-dicarbonyl shown in comparison to the calculated spectrum of pristine PC$_{60}$BM and experimental FTIR data measured for a PC$_{60}$BM film exposed to light in air for 47 hours. Spectra calculated for photodegradation products with complete cages (red, respectively, pink lines), containing 60 C atoms, and fragmented cages (green, respectively, blue lines), containing 58 C atoms, are shown. All calculated spectra have been scaled by a factor 0.9627[2] and shifted by 22 cm^{-1} towards lower wavenumbers to align to the carbonyl peak position measured for pristine PC$_{60}$BM. The spectra are obtained by broadening the calculated bar graphs with Gaussian functions of 10 cm^{-1} FWHM. The peaks are denoted as in the article, where 'S' corresponds to symmetric stretch vibrations, while 'A' correspond to antisymmetric stretch vibrations. The apostrophe marks the peaks calculated for products with complete cages. The insets depict the molecular structures of the four considered photodegradation products, where the cage C atoms at the adsorption site are marked yellow and the side-chains have been omitted for clarity.

REFERENCES

[1] I. E. Brumboiu, A. S. Anselmo, B. Brena, A. Dzwilewski, K. Svensson, and E. Moons, Chem. Phys. Lett. **568**, 130 (2013).

[2] J. P. Merrick, D. Moran, and L. Radom, J. Phys. Chem. A **111**, 11683 (2007).

[3] I. E. Brumboiu, L. Ericsson, R. Hansson, E. Moons, O. Eriksson, and B. Brena, J. Chem. Phys. **142**, 054306 (2015).